Appendix B

Linear Coupled Oscillators with Thermal Noise

Trapped electrons are coupled to a tuned circuit for detection and eventually come into equilibrium with it. The trap electrodes and tuned circuit are in thermal contact with a LHe bath. Thermal motions are observable even near 4 K. For example, the precision of the measured magnetic moment of the electron using a magnetic"bottle" [83] may ultimately be limited by the substantial linewidth broadening caused by the thermal axial motion of an electron in the magnetic field gradient, unless a variable bottle [86] can be used. The thermal motion of an electron oscillator has been thoroughly analyzed [7,10]. In this section, we describe the Johnson noise in the tuned circuit and a square-law detection technique [18,93] used in observing thermal agitations. Some interesting and useful features arising from the interaction between the tuned circuit and trapped electrons are discussed. A simplified explanation is provided for heat transfer in an electron/ion cloud which are sufficiently gradual (quasi-static). Finally, the basic features of a "bolometric" model [18,93] of disordered motions in trapped electrons/ions are summarized.

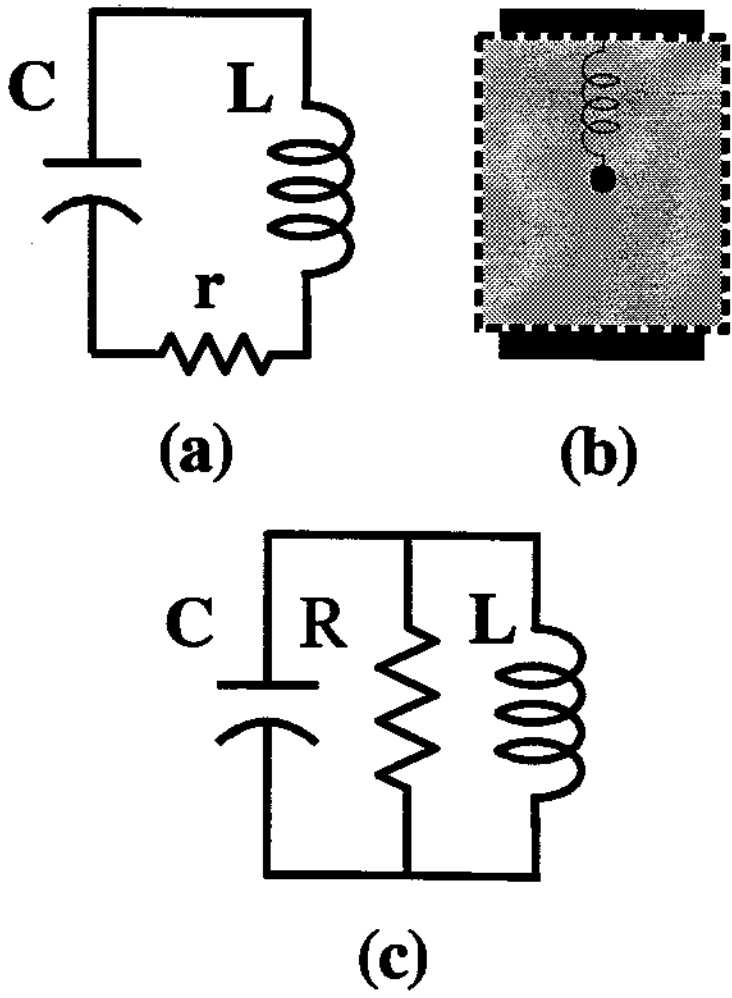

Figure B.1: Harmonic oscillators: (a) series LCr network, (b) damped, ideal spring-mass system, (c) parallel LCR network .

B.1 Detection Circuit: Harmonic Oscillator

The simplest representation of the detection circuit is a series LCr network (represented in Fig. B.1a, where L is the inductance of the helical resonator, C is the trap capacitance, and r represents radio frequency losses in the circuit).

This network is exactly analogous to a damped, harmonic oscillator illustrated in Fig. B.1b consisting of a mass attached to an ideal, massless spring surrounded by a viscous medium. The observed signal is derived from the voltage across the inductor $V_L = L\dot{I}(t)$ where $I(t) = \dot{Q}(t)$ is the current through the inductor. Since thermal agitations produce $\langle V_L(t) \rangle = 0$, only the mean squared value is measured. (The symbol $\langle ... \rangle$ denotes ensemble average.) The mean squared fluctuation in a small frequency bandwidth $\Delta\omega$ can be measured using a square-law detection technique (Fig. 2.15). The theory of square-law detection is briefly discussed in this section.

The voltage across the inductor is amplified, filtered and squared to produce a signal proportional to mean noise power. The signal is obtained by the sum of Fourier amplitudes in the bandpass $[\omega - \Delta\omega/2, \omega + \Delta\omega/2]$of the filter

$$S_N = \int_{-\infty}^{+\infty} dt F(t) V_L(t) \tag{B.1}$$

where the function $F(t)$ which restricts the observation bandwidth,$\Delta\omega$, is given by [10]

$$F(t) = 2 \int_{-\Delta\omega/2}^{+\Delta\omega/2} \frac{d\omega'}{2\pi} cos\left[(\omega_F + \omega')t - \phi\right]. \tag{B.2}$$

The phase ϕ is adjusted by a phase-shifter. Observed output of squarer is proportional to

$$\langle S_N^2 \rangle = \int_{-\infty}^{+\infty} dt_1 \int_{-\infty}^{+\infty} dt_2 F(t_1) F(t_2) \langle V_L(t_1) V_L(t_2) \rangle \ . \tag{B.3}$$

The correlation function for $V_L(t)$ is related to the impedance $\underline{Z}(\omega)$ of the network by [90]

$$\langle V_L(t_1) V_L(t_2) \rangle = 2k_B T r \int_{-\infty}^{+\infty} \frac{d\omega}{2\pi} (\omega L)^2 \left[\underline{Z}^{-1}(\omega) \underline{Z}^{-1}(-\omega)\right] e^{i\omega(t_2 - t_1)} \ . \tag{B.4}$$

For a series LCr network (e.g., Fig. B.1a), the circuit impedance is given by

$$\underline{Z}(\omega) = r + i\omega L + 1/(i\omega C). \tag{B.5}$$

Hence, in the limit of narrow observation bandwidth $\Delta\omega \ll r/L$, we get the familiar result for Johnson noise

$$\langle S_0^2 \rangle = 4k_B T_r \left[\frac{\Delta\omega}{2\pi}\right] R(\omega) \tag{B.6}$$

where the effective resistance $R(\omega)$ is given by

$$R(\omega) = \left[\frac{L}{rC}\right] \frac{\left(\frac{1}{2}\Gamma_M\right)^2}{(\omega_M - \omega)^2 + \left(\frac{1}{2}\Gamma_M\right)^2} \quad . \tag{B.7}$$

The subscript 0 in (S_0^2) indicates that there are no trapped particles. Observed noise power is maximum when the bandpass filter is centered at the resonance frequency ω_M of the tuned circuit. A "noise resonance" is obtained by sweeping the bandpass center frequency, producing a Lorentzian lineshape with resonant frequency $\omega_M = 1/\sqrt{LC}$ and a full width at half-maximum of $\Gamma_M = r/L$. Observed noise-driven resonance for our apparatus is shown in Fig. B.2a, when the trap is empty.

A helical resonator has often been represented by a parallel LCR network shown in Fig.(B.1c) in earlier works [93]. In practice, because the quality factor is fairly high ($Q > 600$), the difference between these two representations is negligible (of order $1/Q$) provided the resistances r and R are related by

$$R = \frac{L}{rC} \quad . \tag{B.8}$$

While the parallel LCR representation is very convenient when $\omega^2 \simeq 1/(LC)$, the series LCr circuit more readily provides a detailed study in general, particularly when the circuit is coupled to trapped particles.

B.2 Coupled oscillators

An electron bound in the trap interacts with the tuned circuit. For a pure electrostatic quadrupole potential, the axial motion of an electron is represented by a spring oscillator. Fig. B.3 illustrates the coupling of the tuned circuit to a trapped electron. In general, the electron may be surrounded by a fluid medium consisting of background gas (e.g., in a poor vacuum) or consisting of simultaneously trapped ions.

The coupling between an electron and the tuned circuit is described by the interaction potential

$$V_{int} = \left[\frac{\kappa q}{dC}\right] ZQ \tag{B.9}$$

where $Z(t)$ is the displacement from the trap center along the symmetry axis and $Q(t)$ is the charge accumulated in the capacitor. The dimensionless geometric

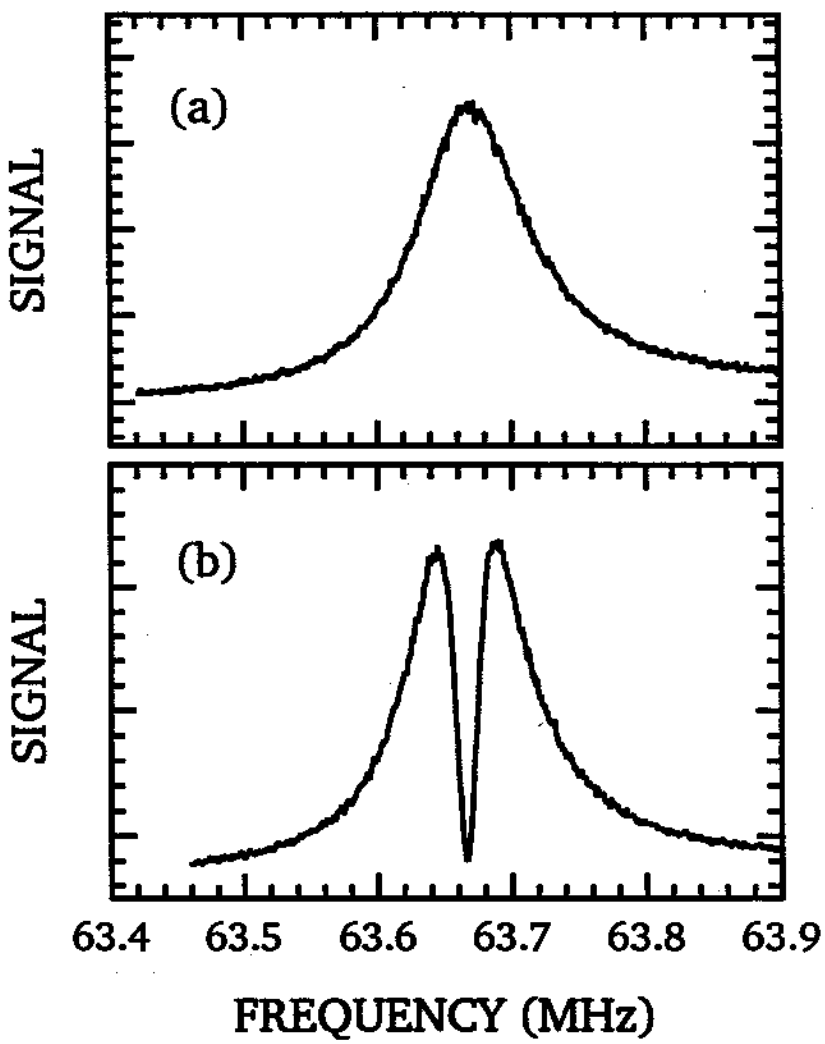

Figure B.2: Observed "noise resonance" of the tuned circuit obtained by sweeping the center frequency of bandpass filter (a) when the trap is empty and (b) when the trap has a small electron cloud with the same resonant frequency.

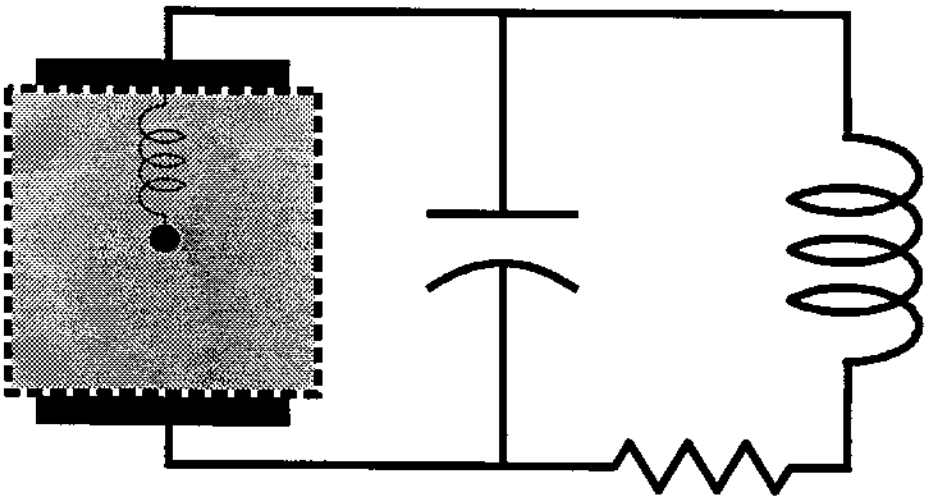

Figure B.3: Simplified representation of a tuned circuit coupled to an charged particle oscillating in a background gas.

factor κ is equal to 1 for an infinite parallel plate capacitor. Thus, the Langevin equations for the coupled oscillators are

$$\begin{aligned} L\left[\frac{d^2}{dt^2}+\Gamma_M\frac{d}{dt}+\omega_M^2\right]Q(t)+\left[\frac{\kappa q}{dC}\right]Z(t) &= V(t), \\ m\left[\frac{d^2}{dt^2}+\gamma_{col}\frac{d}{dt}+\omega_o^2\right]Z(t)+\left[\frac{\kappa q}{dC}\right]Q(t) &= F(t), \end{aligned} \tag{B.10}$$

which appear similar to Eq. (2.39) and Eq.(2.40) except that the "Langevin forces" on the right hand side (and hence $Z(t)$ and $Q(t)$ as well) are stochastic processes. These random forces have Gaussian distributions with $\langle F(t)\rangle = \langle V(t)\rangle = 0$ and are characterized by the correlation functions:

$$\begin{aligned} \langle V(t)F(t')\rangle &= 0, \\ \langle F(t)F(t')\rangle &= 2k_BT_G(m\gamma_{col})\delta(t-t'), \end{aligned}$$

$$\langle V(t)V(t')\rangle \;=\; 2k_BT_r(L\Gamma_M)\delta(t-t'). \tag{B.11}$$

They are uncorrelated, "white" noise sources. In this section, we examine the characteristic features of the observed signal when the system of coupled oscillators is driven by white noise.

Consider first the case of an electron harmonically bound in an ultra-high vacuum envelope held at temperature T. In this case, collisions with background gas is completely negligible, so that $\gamma_{col} = 0$. The output of the squarer given by Eq.(B.6) must be modified to read

$$\langle S_N^2\rangle = \langle S_0^2\rangle \frac{(\omega_z^2-\omega^2)^2}{((\tilde{\omega}_z)^2-\omega^2)^2+(\omega\gamma_z)^2} \tag{B.12}$$

where the $\tilde{\omega}_z$ is the shifted resonant frequency of the electron oscillator and γ_z is its damping rate due to coupling with the circuit , given by Eq.(2.49). The damping and frequency shift caused by the tuned circuit are discussed in Sec. 4, where they are shown to depend in a simple way on the detuning from the tuned circuit.

Features due to this coupling are more easily observed with many electrons since the center-of-mass (CM) motion is also coupled to the tuned circuit in the same way. The description given above remains valid for N electrons suspended near the trap center, provided $q \longrightarrow Nq$, $m \longrightarrow Nm$, and $Z(t)$ becomes the CM coordinate. Illustrative cases calculated from Eq.(B.12) are shown in Fig. B.4.

If the resonant frequencies of the spring oscillator and LCr circuit are tuned to the same value $\omega_z = \omega_M$, a "dip" appears at the center of the signal. An example of observed dip in the noise resonance of the tuned circuit due to trapped electrons is shown in Fig. B.2b. For small number of electrons, $N\gamma_z \ll \Gamma_M$, the signal in a small frequency range about ω_z simplifies to read

$$\langle S_N^2\rangle = 4k_BTR\left(\frac{\Delta\omega}{2\pi}\right)\left[1-\frac{(\Gamma_o/2)^2}{(\omega_z-\omega)^2+(\Gamma_o/2)^2}\right] \quad . \tag{B.13}$$

Thus, the electrons produce an inverted Lorentzian with linewidth $\Gamma_o \equiv \Gamma_z(0) = N\gamma_{zo}$ (i.e., N times wider than the maximum linewidth of one electron). The signal

is "shorted out" at the resonant frequency as shown in Fig.(B.4b). For large N, the signal maxima $\langle S_N^2 \rangle_{max}$ occur at frequencies

$$\omega^{\pm} = \omega_M \pm \frac{1}{2}\sqrt{\Gamma_M \Gamma_o} \quad , \tag{B.14}$$

which are separated by the geometric mean of the widths Γ_o and Γ_M, as can be easily shown by demanding the derivative of Eq.(B.12) with respect to ω to be equal to zero. Thus, $\Gamma_o = (\omega^+ - \omega^-)^2)/\Gamma_M$ can be used to determine N for large systems.

In general, the observed signal is "shorted out" at the unperturbed resonant frequency of the particle oscillator ω_z even when $\omega_z \neq \omega_M$. This feature could be useful for high precision mass spectroscopy which compares ions of nearly the same mass (such as protons and antiprotons) without being limited by shifts caused by the detection circuit. It should be noted that the sharp peak near the ω_z has its maximum slightly farther away from the tuned circuit resonant frequency than $\tilde{\omega}_z$. In the narrowband limit, this maximum occurs at

$$\omega_{max} = \tilde{\omega}_z + \frac{N\gamma_z}{2}\left[\frac{\Gamma_M/2}{\omega_z - \omega_M}\right] \quad . \tag{B.15}$$

The order in the frequencies is given by

$$\begin{aligned} &\omega_M < \omega_z < \tilde{\omega}_z < \omega^+ \quad for \quad \omega_z > \omega_M \quad , \\ &\omega^- < \tilde{\omega}_z < \omega_z < \omega_M \quad for \quad \omega_M > \omega_z \quad , \end{aligned} \tag{B.16}$$

as illustrated in Fig. B.4c.

B.3 Electron Cooling of Trapped Antiprotons

Fig. B.3 provides a simple model for the process of cooling antiprotons captured in a Penning trap using simultaneously trapped electrons sharing the same trapping volume. [35] Consider one electron trapped together with a hot cloud of anti-protons. If spontaneous emission is completely suppressed, then the electron couples only to the LCr circuit connected to the trap electrodes. Without

the tuned circuit, the electron comes into equilibrium with the antiproton gas at temperature T_G and undergoes brownian motion. When the tuned circuit is connected to the electrodes, the electron couples and transfers energy to the tuned circuit which dissipates the energy in the resistor. This process gradually cools the antiproton gas surrounding the electron.

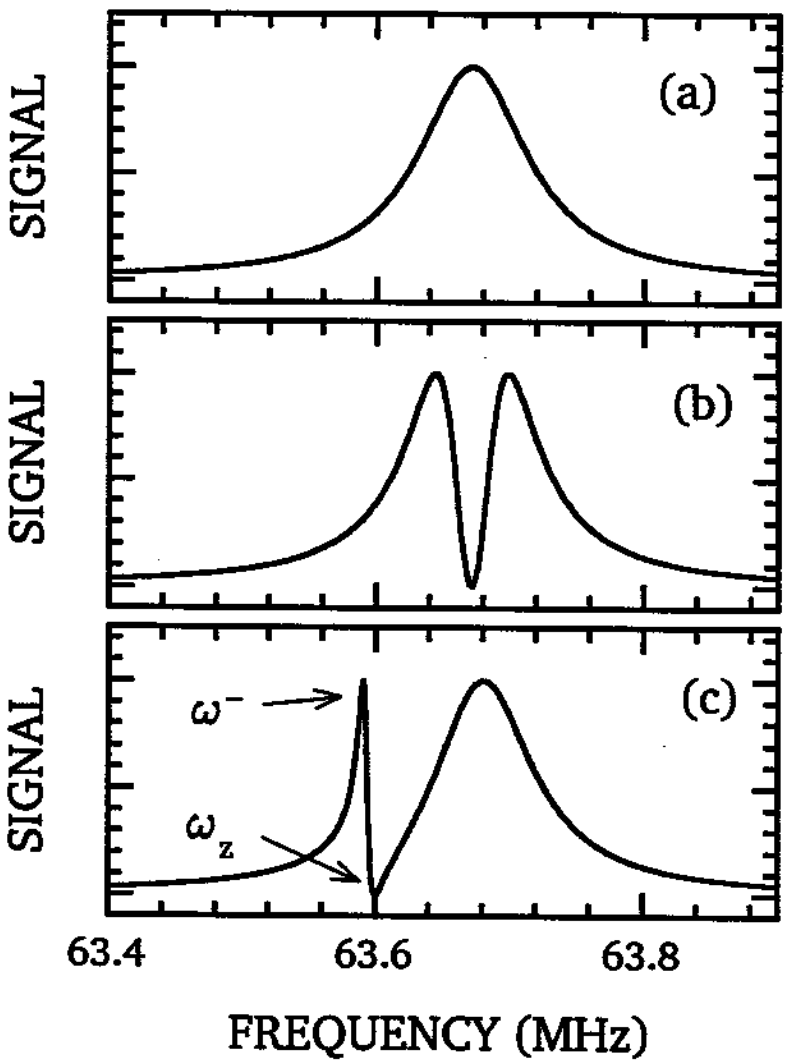

Figure B.4: Calculated noise power from tuned circuit coupled to (a) no electron, (b) small electron cloud at $\omega_z = \omega_M$, and (c) small electron cloud at $\omega_z > \omega_M$

The rate of cooling is equal to the power dissipated in the resistor. If the process is quasi-static, then we can write

$$C_G \frac{d}{dt} T_G \;=\; -\langle \dot{Q}(t)^2 \rangle r, \tag{B.17}$$

where C_G is the heat capacity of the gas. Joule heating (right hand side) can be calculated from the fluctuating current in the tuned circuit induced by the Brownian motion of the electron oscillator (which is driven by the heat bath of antiprotons). This has a simple form when $\gamma_{col} + \gamma_z \ll \Gamma_M$:

$$\langle \dot{Q}(t)^2 \rangle r = \left(\frac{\gamma_{col}\gamma_z}{\gamma_{col} + \gamma_z} \right) k_B T_G \;\;, \tag{B.18}$$

where γ_z is the decay rate of electron oscillation due to the tuned circuit. At sufficiently high temperature, the heat capacity C_G is independent of temperature. Hence, the temperature of the antiprotons gas drop exponentially with a damping constant τ given by

$$\frac{1}{\tau} = \frac{k_B}{C_G} \left(\frac{\gamma_{col}\gamma_z}{\gamma_{col} + \gamma_z} \right). \tag{B.19}$$

Typically,the damping rate γ_z of an electron by a tuned circuit is sufficiently fast near resonance, and hence the cooling rate of the antiprotons is essentially determined by the collision constant γ_{col} and the heat capacity. That is, for $\Gamma_M \gg \gamma_z \gg \gamma_{col}$, the cooling rate is $\tau^{-1} = \gamma_{col}(k_B/C_G)$. If now we sweep the cyclotron frequency into resonance with a cavity mode, then a factor of 2 in cooling rate is gained from synchrotron radiation provided energy transfer to the electron cyclotron motion has the same time constant. On the other hand, unavoidable anharmonicity in real Penning traps makes large axial motions very anharmonic. This would cause the electron oscillator to be greatly detuned from the cold, LCr circuit so that $\gamma_z \ll \gamma_{col}$, thus making the cooling process much less efficient. Since the heat capacity is proportional to the number of gas particles, a large number of electrons is necessary to get useful cooling rates.

This description of electron cooling of trapped antiprotons , although qualitatively useful, is oversimplified in some important aspects. For example, the equilibration time constant between electrons and anti-protons is a function of tempera-

ture and density. Furthermore, the heat capacity of a cloud of harmonically-bound antiprotons is different from that of a gas. Careful consideration of such issues is given in Ref. [72].

B.4 Bolometric model

In addition to the coupling between CM motion and tuned circuit, an electron cloud has many internal degrees of freedom which can be heated separately with an RF or microwave drive. The electron cloud gyrates in the strong magnetic field of the Penning trap and thus can radiate via cavity modes which couple to the cyclotron motion, just as the axial CM motion is damped by the tuned circuit. A full description of the dynamics is difficult. The problem is significantly simplified if the disordered, internal motions of a given type (e.g., axial oscillations) form a thermal reservoir characterized by a temperature. A "bolometric" model [18,93] of trapped electrons/ions has been developed which essentially focuses on the temperatures of such reservoirs. To illustrate the main features of the bolometric model, we first consider a simple example, which can be generalized.

The simplified system is made up of only the axial motions of the electrons ($B \rightarrow \infty$ limit). For a pure electrostatic quadrupole potential, the axial CM motion is completely decoupled from the thermal reservoir formed by the internal motions. In practice, however, deviations from the pure electrostatic quadrupole couple the CM motion to the internal reservoir. Fig. B.3 can be used for illustration if the "gas" now represents the internal (axial) degrees of freedom of the electron cloud. The tuned circuit is assumed to be held at a temperature T_r, and an amount of power $\dot{H}$ flowing through the container heats or cools this "gas".

Under quasi-static conditions, energy conservation requires that

$$C_G \frac{d}{dt} T_G = \dot{H} + (m\gamma_{col})\langle \dot{Z}^2 \rangle - \langle \dot{Q}(t)^2 \rangle r. \qquad \text{(B.20)}$$

where we have added two more terms to Eq.(B.17) . The term $(m\gamma_{col})\langle \dot{Z}^2 \rangle$ accounts for the heat dissipated in the gas by the axial oscillation $Z(t)$, which is driven by

the Johnson noise in the tuned circuit. Joule heating in the tuned circuit is given by $\langle \dot{Q}^2 \rangle r$. The term $\dot{H}$ is due to heat exchange between the gas and the external world. Mean squared terms on the right hand side can be calculated to give

$$C_G \frac{d}{dt} T_G = g(T_r - T_G) + \dot{H}. \tag{B.21}$$

The thermal conductivity between the internal reservoir and the resistor r via the brownian motions of the coupled oscillators is given by

$$g = 2k_B \gamma_{col} \Gamma_o (\Gamma_M \omega_M)^2 \int \frac{d\omega}{2\pi} \left| \frac{\omega}{\Delta} \right|^2 \tag{B.22}$$

where

$$\Delta \equiv (\omega_M^2 - \omega^2 - i\Gamma_M \omega)(\omega_z^2 - \omega^2 - i\gamma_{col}\omega) - \Gamma_M \omega_M^2 \Gamma_o \ . \tag{B.23}$$

This integral has a simple limit if $\Gamma_M \gg \gamma_{col} + \Gamma_z$, yielding $g = k_B \gamma_{col} \Gamma_z / (\gamma_{col} + \Gamma_z)$ with Γ_z being the damping rate of the CM motion due to the tuned circuit. This is one of the simplest case of the bolometric model.

We summarize here the basic features of the bolometric model, represented electro-mechanically in Fig.(B.5). Two internal reservoirs are used to account for both axial and cyclotron motions. For parallel motions, a tuned circuit is coupled to the axial CM motion , which in turn interacts with the gas representing the internal axial motions of the electron cloud. For transverse motions, a cavity mode (represented by an LCr circuit) is coupled to the cyclotron CM motion, which in turn interacts with another reservoir representing the cyclotron internal motions . Heat exchange between the internal reservoirs occurs via electron-electron collisions. External sources can raise the temperatures of these motions independently.

Assuming that equilibration time between the internal reservoirs is shorter than other relaxation times, further simplification is obtained by combining all internal motions into one reservoir at temperature T_i. The two temperatures of interest are those of the axial CM motion T_z and the temperature of the combined internal reservoir T_i. Energy conservation gives a system of first-order ordinary differential equations [18,93]

$$C_z \frac{d}{dt} T_z = g_{rz}(T_r - T_z) + g_{iz}(T_i - T_z) + \dot{H}_z,$$

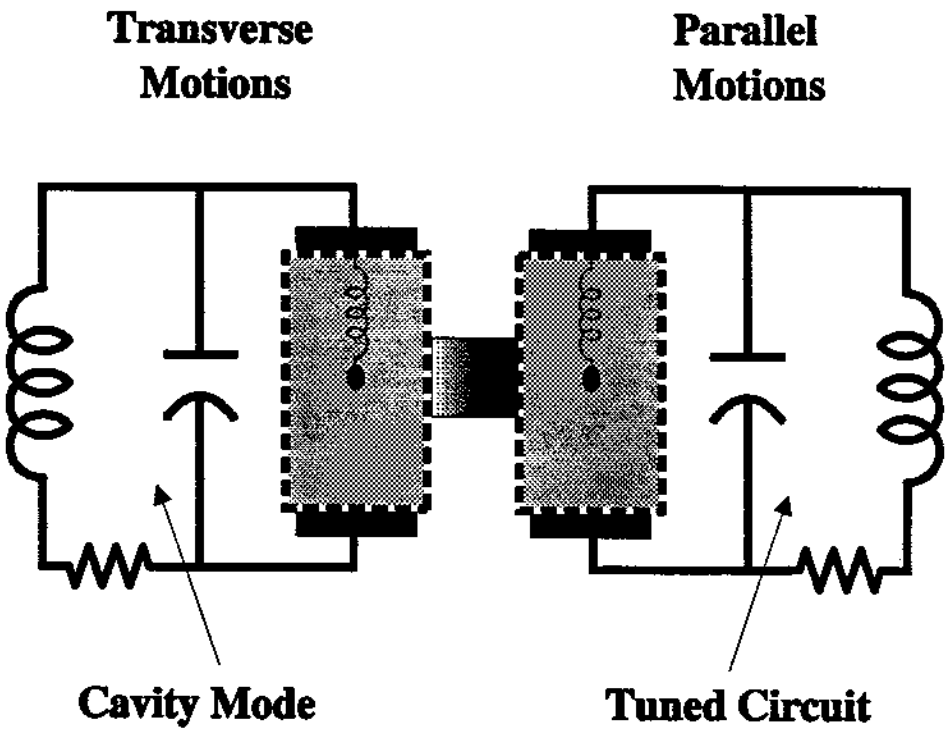

Figure B.5: The bolometric model

$$C_i \frac{d}{dt} T_i \quad = \quad g_{Mi}(T_M - T_i) + g_{zi}(T_z - T_i) + \dot{H}_i, \tag{B.24}$$

where T_r and T_M are the temperatures of the detection circuit and cavity, respectively. (Typically, $T_r \approx T_M$.) The terms $\dot{H}_z$ and $\dot{H}_i$ denote energy flowing into the axial CM motion and internal reservoir, respectively. The heat capacities C_z and C_i are those for harmonic oscillators (k_B per oscillator). The thermal conductivities g_{ij} are determined experimentally. This set of rate equations has been thoroughly investigated with trapped electrons cooled to $\sim$ 80K, for which the equilibration time between internal reservoirs is observed to be very fast. [93] The

equilibration rate, however, can decrease dramatically at much lower temperatures [68] and a more general set of rate equations may be necessary. Finally, the bolometric model is useful only if the system is not driven so strongly that collective behaviors emerge.